Cell Communication and Signaling

RESEARCH

Open Access

PPARβ/δ upregulates the insulin receptor β subunit in skeletal muscle by reducing lysosomal activity and EphB4 levels

Jue-Rui Wang[1,2,3†], Javier Jurado-Aguilar[1,2,3†], Emma Barroso[1,2,3], Ricardo Rodríguez-Calvo[2,4], Antoni Camins[1,5,6], Walter Wahli[7,8], Xavier Palomer[1,2,3] and Manuel Vázquez-Carrera[1,2,3,9*]

Abstract

Background The increased degradation of the insulin receptor β subunit (InsRβ) in lysosomes contributes to the development of insulin resistance and type 2 diabetes mellitus. Endoplasmic reticulum (ER) stress contributes to insulin resistance through several mechanisms, including the reduction of InsRβ levels. Here, we examined how peroxisome proliferator-activated receptor (PPAR)β/δ regulates InsRβ levels in mouse skeletal muscle and C2C12 myotubes exposed to the ER stressor tunicamycin.

Methods Wild-type (WT) and *Ppard*$^{-/-}$ mice, WT mice treated with vehicle or the PPARβ/δ agonist GW501516, and C2C12 myotubes treated with the ER stressor tunicamycin or different activators or inhibitors were used.

Results *Ppard*$^{-/-}$ mice displayed reduced InsRβ protein levels in their skeletal muscle compared to wild-type (WT) mice, while the PPARβ/δ agonist GW501516 increased its levels in WT mice. Co-incubation of tunicamycin-exposed C2C12 myotubes with GW501516 partially reversed the decrease in InsRβ protein levels, attenuating both ER stress and the increase in lysosomal activity. In addition, the protein levels of the tyrosine kinase ephrin receptor B4 (EphB4), which binds to the InsRβ and facilitates its endocytosis and degradation in lysosomes, were increased in the skeletal muscle of *Ppard*$^{-/-}$ mice, with GW501516 reducing its levels in the skeletal muscle of WT mice.

Conclusions Overall, these findings reveal that PPARβ/δ activation increases InsRβ levels by alleviating ER stress and lysosomal degradation.

Keywords PPARβ/δ, InsRβ, EphB4, ER stress, GW5101516

†Jue-Rui Wang and Javier Jurado-Aguilar contributed equally to this work.

*Correspondence:
Manuel Vázquez-Carrera
mvazquezcarrera@ub.edu
[1]Department of Pharmacology, Toxicology and Therapeutic Chemistry, Faculty of Pharmacy and Food Sciences, Institute of Biomedicine of the University of Barcelona (IBUB), University of Barcelona, Barcelona 08028, Spain
[2]Spanish Biomedical Research Center in Diabetes and Associated Metabolic Diseases (CIBERDEM)-Instituto de Salud Carlos III, Madrid 28029, Spain
[3]Pediatric Research Institute-Hospital Sant Joan de Déu, Esplugues de Llobregat, Spain
[4]Vascular Medicine and Metabolism Unit, Research Unit on Lipids and Atherosclerosis, "Sant Joan" University Hospital, Universitat Rovira i Virgili, Pere Virgili Health Research Institute (IISPV), Reus 43201, Spain
[5]Biomedical Research Networking Centre in Neurodegenerative Diseases (CIBERNED), Madrid, Spain
[6]Institute of Neuroscience, University of Barcelona, Barcelona, Spain
[7]Center for Integrative Genomics, University of Lausanne, Lausanne CH-1015, Switzerland
[8]INRAE ToxAlim, UMR1331, Chemin de Tournefeuille, Toulouse Cedex 3 F-31027, France
[9]Unitat de Farmacologia, Facultat de Farmàcia i Ciències de l'Alimentació, Av. Joan XXIII 27-31, Barcelona E-08028, Spain

Background

Insulin resistance, which can be defined as a defect in the capacity of insulin to drive glucose into its target tissues, predicts and precedes the development of type 2 diabetes mellitus (T2DM) [1]. Skeletal muscle accounts for most of the insulin-stimulated glucose use and, thus, is the primary tissue affected by insulin resistance [2]. Insulin signaling is initiated when the hormone binds to the α subunit of the insulin receptor (InsRα), which derepresses the tyrosine kinase activity of the β subunit (InsRβ). The InsRβ then phosphorylates InsR substrate (IRS) molecules at tyrosine residues. Insulin signaling then proceeds through the activation of several components, including phosphoinositide 3-kinase (PI3K), Akt, and Akt substrate of 160 kDa (AS160), to promote glucose uptake via glucose transporter type 4 (GLUT4) [3]. A decrease in the cell surface presentation of InsR and its tyrosine kinase activity is one of the main factors contributing to dysregulated insulin signaling and insulin resistance [4]. However, the mechanisms involved in InsR downregulation have only been partially explored.

Several factors contribute to the reduced InsR levels that provoke insulin resistance. Hyperinsulinemia in insulin resistance and T2DM has been reported to increase the proteasomal and lysosomal degradation of the InsRβ in podocytes, attenuating insulin signaling [5]. Likewise, InsR levels are negatively associated with the levels of the endoplasmic reticulum (ER) stress marker C/EBP homologous protein (CHOP) in the insulin target tissues of *db/db* mice and mice fed a high-fat diet (HFD) [6]. Moreover, InsR is downregulated in the adipose tissue of obese human subjects and in cultured adipocytes treated with ER stressors [6]. ER stress also depletes InsR at the plasma membrane by inhibiting the delivery of newly synthesized insulin receptors to the cell surface [7]. Interestingly, a recent finding documented the interaction of the InsRβ with ephrin receptor B4 (EphB4), a tyrosine kinase receptor that modulates cell adhesion and migration, in a process stimulated by insulin that facilitates clathrin-mediated InsR endocytosis and degradation in lysosomes [8].

The nuclear receptor peroxisome proliferator-activated receptor β/δ (PPARβ/δ) regulates glucose and lipid metabolism, as well as inflammation. In fact, PPARβ/δ agonists attenuate dyslipidemia and hyperglycemia, improve whole-body insulin sensitivity and prevent HFD-induced obesity [9]. PPARβ/δ is required in the skeletal muscle to maintain slow oxidative fibers. Furthermore, the skeletal muscle-specific deletion of PPARβ/δ in mice leads to obesity and diabetes [10]. We have previously reported that the PPARβ/δ agonist GW501516 increases the protein levels of the InsRβ in skeletal muscle [11]. Others have found that GW501516 increases the protein levels of InsR and prevents the reduction of its levels caused by tumor necrosis factor α (*Tnfα*) in cultured adipocytes [12]. However, the mechanisms by which PPARβ/δ activation upregulates InsR levels remain unknown. Here, we show that the protein levels of the InsRβ are reduced in the skeletal muscle of *Ppard*$^{-/-}$ mice compared to wild-type (WT) mice. By contrast, the PPARβ/δ agonist GW501516 increases InsRβ protein levels in the skeletal muscle of WT mice. In addition, GW501516 attenuates the reduction of InsRβ protein levels caused by the ER stressor tunicamycin in C2C12 myotubes and also reduces the tunicamycin-induced increase in lysosomal activity. Furthermore, EphB4 protein levels are increased in the skeletal muscle of *Ppard*$^{-/-}$ mice, with GW501516 reducing its levels in WT mice. Altogether, these findings indicate that PPARβ/δ activation in skeletal muscle prevents the ER stress-mediated reduction in InsRβ levels by attenuating ER stress and lysosomal activity, as well as by reducing EphB4-mediated degradation in lysosomes.

Methods

Reagents

GW501516 (SML1491) and chloroquine (C6628) were purchased from Sigma-Aldrich Corporation (St. Louis, MO, USA). Tunicamycin (#3516) was obtained from Bio-Techne R&D Systems (Minneapolis, MN, USA), while nutlin-3 (sc-45061) and A769662 (sc-203790) were purchased from Santa Cruz Biotechnology (Dallas, TX, USA).

Mice

Male (8–9 weeks old) *Ppard*-knockout (*Ppard*$^{-/-}$) mice (n=5) and their WT littermates (*Ppard*$^{+/+}$) (n=5) with the same genetic background (C57BL/6×129/SV) (12), all fed a control diet, were housed and maintained under a constant temperature (22±2 °C) and humidity (55%). No significant differences were observed in body weight or food intake between WT and *Ppard*$^{-/-}$*mice*. The mice were sacrificed, and skeletal muscle samples were frozen in liquid nitrogen before being stored at -80ºC.

In another study, male C57BL/6 mice (10–12 weeks old) (Envigo, Barcelona, Spain) were housed and maintained under a constant temperature (22±2 °C) and humidity (55%). The mice had free access to water and food and were subjected to 12-h light-dark cycles. After 1 week of acclimatization, the mice were randomly distributed into two experimental groups (n=5 each): one group received one daily p.o. gavage of vehicle (0.5% w/v carboxymethylcellulose) for 6 consecutive days, while the other group received 3 mg/kg/day of GW501516 dissolved in the vehicle (volume administered, 1 mL/kg). No significant changes in food intake or body weight were observed throughout the treatment. At the end of the treatment, the mice were sacrificed. Samples of their

skeletal muscle (*gastrocnemius*) and epididymal adipose tissue were frozen in liquid nitrogen and then stored at -80ºC.

All experiments were performed in accordance with the European Community Council directive 86/609/EEC. The experimental protocols and the number of animals, determined based on the expected effect size, were approved by the Institutional Animal Care and Use Committee of the University of Barcelona. The reporting of the animal studies complied with the ARRIVE guidelines. Accordingly, all efforts were made to minimize the suffering and the number of mice used.

Cell culture

Mouse C2C12 myoblasts (ATCC) were maintained in Dulbecco's modified Eagle's medium (DMEM) supplemented with 10% fetal bovine serum (FBS), 50 units/mL of penicillin, and 50 mg/mL of streptomycin. When cells reached confluence, the medium was switched to the differentiation medium containing DMEM and 2% horse serum, which was changed every other day. After four more days, the differentiated C2C12 cells had fused into myotubes. These were incubated in serum-free DMEM in either the absence (control cells) or presence of the following concentrations of tunicamycin (0.1–5 μg/mL) [13], GW501516 (10 μM), a concentration that selectively activates PPARβ/δ [14], A769662 (60 μM) [15] or chloroquine (50 μM) [16]. Treatment with these compounds did not significantly reduce cell viability (Supplementary Fig. 1) assessed by the thiazolyl blue tetrazolium bromide (MTT) assay (M2128, Sigma-Aldrich Corporation). All the cell experiments were repeated at least three times and there were two replicates in each experiment.

Reverse transcription-polymerase chain reaction and quantitative polymerase chain reaction

Isolated RNA was reverse transcribed to obtain 1 μg of complementary DNA (cDNA) using Random Hexamers (Thermo Fisher Scientific, Waltham, MA, USA), 10 mM of the deoxynucleotide (dNTP) mix and the reverse transcriptase enzyme derived from the Moloney murine leukemia virus (MMLV, Thermo Fisher Scientific). cDNA synthesis was run in a thermocycler (Bio-Rad, Hercules, CA, USA) and consisted of a program with different steps and temperatures: 65 °C for 5 min, 4 °C for 5 min, 37 °C for 2 min, 25 °C for 10 min, 37 °C for 50 min, and 70 °C for 15 min. The relative levels of specific mRNAs were assessed by real-time RT-PCR in a Mini 48-Well T100™ thermal cycler (Bio-Rad), using the SYBR Green Master Mix (Applied Biosystems, Waltham, MA, USA), as previously described [17]. Briefly, samples had a final volume of 20 μL, with 20 ng of total cDNA, 0.9 μM of the primer mix, and 10 μL of 2x SYBR Green Master Mix. The thermal cycler protocol for real-time PCR included the first step of denaturation at 95 °C for 10 min followed by 40 repeated cycles of 95 °C for 15 s, 60 °C for 30 s, and 72 °C for 30 s for denaturation, primer annealing, and amplification, respectively. Primer sequences were designed using the Primer-BLAST tool (NCBI), based on the full mRNA sequences to find the optimal primers for amplification, and evaluated with the Oligo-Analyzer tool (Integrated DNA Technologies, Coralville, IA, USA) to ensure an optimal melting temperature (Tm) and avoid the formation of homo/heterodimers or non-specific structures that can interfere with the interpretation of the results. The primer sequences were designed specifically to span the junction between the exons. The primer sequences used are provided in Supplementary Table 1. Values were normalized to the expression levels of glyceraldehyde 3-phosphate dehydrogenase (*Gapdh*), and measurements were performed in triplicate. All changes in expression were normalized to the untreated control.

Immunoblotting

The isolation of total protein extracts was performed as described elsewhere [11]. Immunoblotting was performed with antibodies against AMPKα (#2532, Cell Signaling Technology, Danvers, MA, USA), phospho-AMPKα Thr172 (#2531, Cell Signaling Technology), ATF4 (sc-390063, Santa Cruz Biotechnology), β-actin (A5441, Sigma-Aldrich Corporation), CHOP (GTX112827, GeneTex, Irvine, CA, USA), EphB4 (#37-1800, Invitrogen, Waltham, MA, USA), GAPDH (sc-365062, Santa Cruz Biotechnology), InsRβ (#3052, Cell Signaling Technology), NQO1 (sc-393736, Santa Cruz Biotechnology), p53 (#2524, Cell Signaling Technology), p62 (sc-48402, Santa Cruz Biotechnology), PPARβ/δ (sc-74517, Santa Cruz Biotechnology), and vinculin (sc-73614, Santa Cruz Biotechnology). Secondary antibodies (goat anti-rabbit #1705046 and goat anti-mouse #1705047) were obtained from Bio-Rad. The working dilutions were 1:1,000 (except 1:2,000 for GAPDH, β-actin and vinculin) for primary antibodies and 1:5000 for secondary antibodies. Signal acquisition was conducted using the Bio-Rad ChemiDoc apparatus, while quantification of the immunoblot signal was performed using the Bio-Rad Image Lab software. The results for protein quantification were normalized to the levels of a control protein (GAPDH, vinculin or β-actin) by reprobing the blots to avoid unwanted sources of variation.

Lysosomal activity assay

The lysosomal intracellular activity was measured in C2C12 myotubes using the dye LysoBrite™ Red (AAT Bioquest®, Inc., Pleasanton, CA, USA). The dye working solution was prepared by diluting 20 μL of the 500× LysoBrite™ stock in 10 mL of the medium without phenol red and without L-glutamine. After exposure of the C2C12

myotubes to tunicamycin (0.1 µg/mL) in the presence or absence of 10 µM of GW501516 (PPARβ/δ agonist) for 24 h, the supernatant was removed and the working solution was applied at 100 µL/well. After that, the cells were incubated (37 °C, 5% CO_2; 30 min) and washed twice with medium without phenol red and without L-glutamine. The fluorescence intensity was determined at the excitation and emission wavelengths of 575 and 605 nm, respectively, using the Cytation™ 3 microplate reader (BioTek Instruments GmbH, Sursee, Switzerland).

Statistical analysis

Results are expressed as the mean ± *SD*. Significant differences were assessed by either Student's t-test or ANOVA, according to the number of groups being compared, using the GraphPad Prism program (version 9.0.2) (GraphPad Software Inc., San Diego, CA, USA). When ANOVA found significant variations, Tukey's post-hoc test for multiple comparisons was performed only if F achieved a p-value < 0.05. Differences were considered significant at $p < 0.05$.

Results

Ppard$^{-/-}$ mice show reduced InsRβ protein levels in their skeletal muscle, while the PPARβ/δ agonist GW501516 increases its levels in WT mice

We have previously reported that *Ppard*$^{-/-}$ display glucose intolerance compared to WT mice [18], but the mechanisms involved have not been completely uncovered. We examined InsRβ levels in the skeletal muscle of WT and *Ppard*$^{-/-}$ mice (confirmed by *Ppard* mRNA quantification; Fig. 1A) to evaluate its potential contribution to these differences. *Ppard*$^{-/-}$ mice displayed a reduction in InsRβ protein levels compared with WT mice (Fig. 1B). In line with the reported negative association between InsR levels and the levels of the ER stress marker CHOP [6], we observed that the reduction of InsRβ levels was accompanied by an increase in CHOP levels (Fig. 1B). Overexpression of NAD(P)H: quinone oxidoreductase 1 (NQO1), a target gene of nuclear factor erythroid-2-related factor 2 (Nrf2), has been reported to reduce InsRβ levels in skeletal muscle [19]. *Ppard*$^{-/-}$ mice showed an increase in the levels of the NQO1 protein (Fig. 1B). However, since ER stress increases the expression of Nrf2 and *NQO1* [20], the increase in NQO1

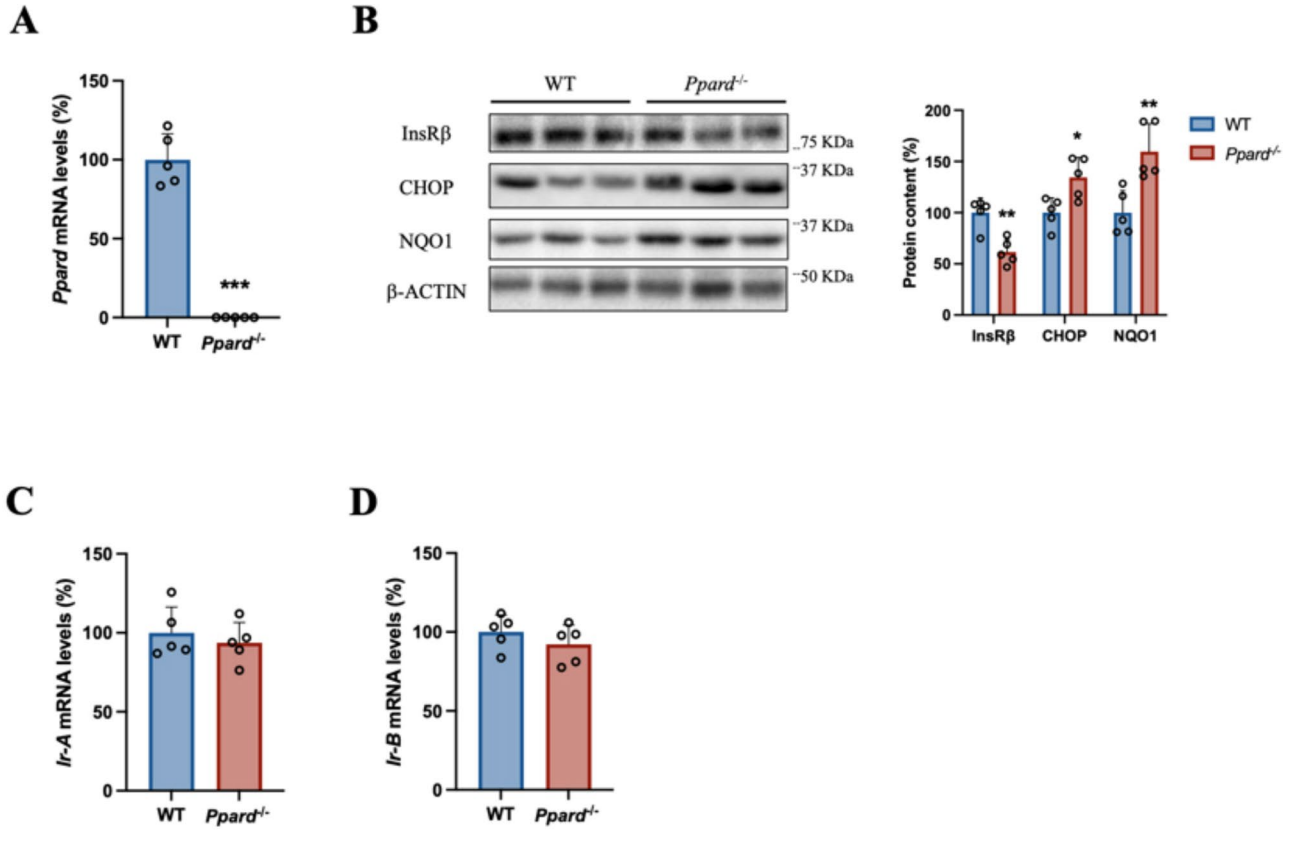

Fig. 1 InsRβ protein levels are reduced in the skeletal muscle of *Ppard*$^{-/-}$ mice. (**A**) mRNA levels of *Ppard* in the skeletal muscle of *Ppard*$^{-/-}$ and WT mice ($n = 5$ animals). (**B**) Skeletal muscle cell lysate extracts from *Ppard*$^{-/-}$ and WT mice were assayed via western blot analysis with antibodies against InsRβ, CHOP, NQO1 or β-actin ($n = 5$ animals). mRNA levels of (**C**) *Ir-A* and (**D**) *Ir-B* in the skeletal muscle of *Ppard*$^{-/-}$ and WT mice ($n = 5$ animals). Data are presented as the mean ± SD. *$p < 0.05$, **$p < 0.01$, and ***$p < 0.001$ *versus* WT. p-values were determined by two-tailed unpaired Student's t-test

protein levels might be due to ER stress in the skeletal muscle of *Ppard*$^{-/-}$ mice. To elucidate whether *Ppard* deficiency led to a reduction in InsRβ levels through a transcriptional mechanism, we assessed the transcript levels of the InsR. The InsR exists as two mRNA species, *Ir-A* and *Ir-B*, derived from the alternative splicing of exon 11 [21]. In the skeletal muscle of *Ppard*$^{-/-}$ mice, the levels of *Ir-A* (Fig. 1C) and *Ir-B* (Fig. 1D) were not significantly reduced, suggesting that the changes observed in InsRβ protein levels occurred at the post-transcriptional level. To confirm that PPARβ/δ activation regulates InsRβ levels in skeletal muscle, we treated mice with the PPARβ/δ agonist GW501516 for 6 days. As expected, GW501516 increased the expression of the well-known PPARβ/δ-target gene pyruvate dehydrogenase kinase 4 (Pdk4) in the skeletal muscle (Fig. 2A). Of note, GW501516 also increased InsRβ protein levels in the skeletal muscle (Fig. 2B). Given that the InsR has been reported to be regulated by p53 [22], we also measured p53 protein levels. GW501516 increased the levels of p53 in skeletal muscle, suggesting that this protein might be involved in the increase in InsRβ levels caused by PPARβ/δ activation (Fig. 2B). The increase in InsRβ levels was accompanied by a slight increase in the levels of p62, a protein degraded via autophagy and lysosomal pathways [23] (Fig. 2C). As mentioned above, ER stress also stimulates the degradation of the InsR [6], which is consistent with GW501516 reducing the levels of the ER stress markers CHOP and activating transcription factor 4 (ATF4) (Fig. 2C). The effect of GW501516 on the InsRβ was not restricted to skeletal muscle, since it was also observed in other tissues such as the white adipose tissue (Fig. 2D). GW501516 also showed a trend to increase p62 protein levels in adipose tissue (Fig. 2D). Altogether, these findings suggest that PPARβ/δ is involved in regulating InsRβ protein levels in skeletal muscle through a post-transcriptional mechanism that might involve a reduction in ER stress.

PPARβ/δ activation partially prevents the ER stress-induced reduction in InsRβ protein levels

Since ER stress reduces InsR protein levels [6], we next examined whether the ER stressor tunicamycin reduced InsRβ levels by attenuating PPARβ/δ levels in C2C12 myotubes. As expected, tunicamycin caused a decrease in PPARβ/δ levels and a remarkable reduction in InsRβ protein levels that were accompanied by an increase in CHOP levels (Fig. 3A). Furthermore, tunicamycin reduced the phosphorylated levels of AMPK, which is consistent with the decrease in PPARβ/δ levels since this nuclear receptor activates AMPK phosphorylation [9, 11]. Interestingly, pre-incubation with GW501516 partially reversed the tunicamycin-induced reduction in the protein levels of the InsRβ and PPARβ/δ in C2C12 myotubes (Fig. 3B, C). These changes were accompanied by a reduction in CHOP protein levels in the cells co-incubated with tunicamycin and GW501516 (Fig. 3D). Since many of the effects of PPARβ/δ are mediated by the phosphorylation of AMPK [9], whose activation prevents ER stress [24], we examined whether the AMPK activator A769662 was able to mimic the effects of GW501516. A769662 did not significantly increase InsRβ protein levels (Fig. 3E). However, the levels of phosphorylated AMPK were increased, indicating that the treatment was effective (Fig. 3E). Likewise, A769662 did not affect p62 protein levels (Fig. 3E). Finally, we examined the effects of A769662 in the presence of tunicamycin. Treatment with A769662 caused a slight recovery in the protein levels of the InsRβ that did not reach statistical significance (Fig. 3F). Since PPARβ/δ activation increases p53 levels [11] and given that p53 is involved in the upregulation of the InsR [22], we examined its potential involvement in the upregulation by GW501516 in C2C12 myotubes. To this end, we treated cells with nutlin 3, a small-molecule inhibitor that binds preferentially to the p53-binding pocket of murine double minute 2 (MDM2). MDM2 is an E3 ubiquitin ligase that mediates the ubiquitination of p53 and targets it for proteasomal degradation [25]. Therefore, MDM2 inhibition by nutlin-3 leads to the stabilization of p53. As expected, exposure of the cells to nutlin-3 increased the protein levels of p53, but this increase did not prevent the downregulation of InsRβ protein levels caused by tunicamycin (Fig. 3F). These findings suggest that neither AMPK activation nor the upregulation of p53 is involved in the beneficial effects of PPARβ/δ activation on the tunicamycin-induced reduction of InsRβ levels.

PPARβ/δ activation prevents the increase in lysosomal activity caused by ER stress

Hyperinsulinemia increases the lysosomal degradation of the InsRβ, which is reversed by co-incubating the cells with an inhibitor of lysosomal degradation [5]. We used the lysosome inhibitor chloroquine to examine whether lysosomal degradation was involved in the reduction of InsRβ levels caused by ER stress in C2C12 myotubes. Interestingly, chloroquine prevented the decrease in InsRβ protein levels caused by tunicamycin (Fig. 4A), indicating that lysosomal degradation is involved in this reduction. The efficacy of chloroquine in inhibiting lysosomal degradation was confirmed by the increase in the protein levels of p62, which is degraded by lysosomal and autophagy pathways [23]. GW501516 also increased p62 levels (Fig. 4B), suggesting that PPARβ/δ activation might prevent the increase in lysosomal activity caused by ER stress. Consistent with this hypothesis, tunicamycin increased lysosomal activity, while co-incubation with GW501516 reversed this increase (Fig. 4C), explaining

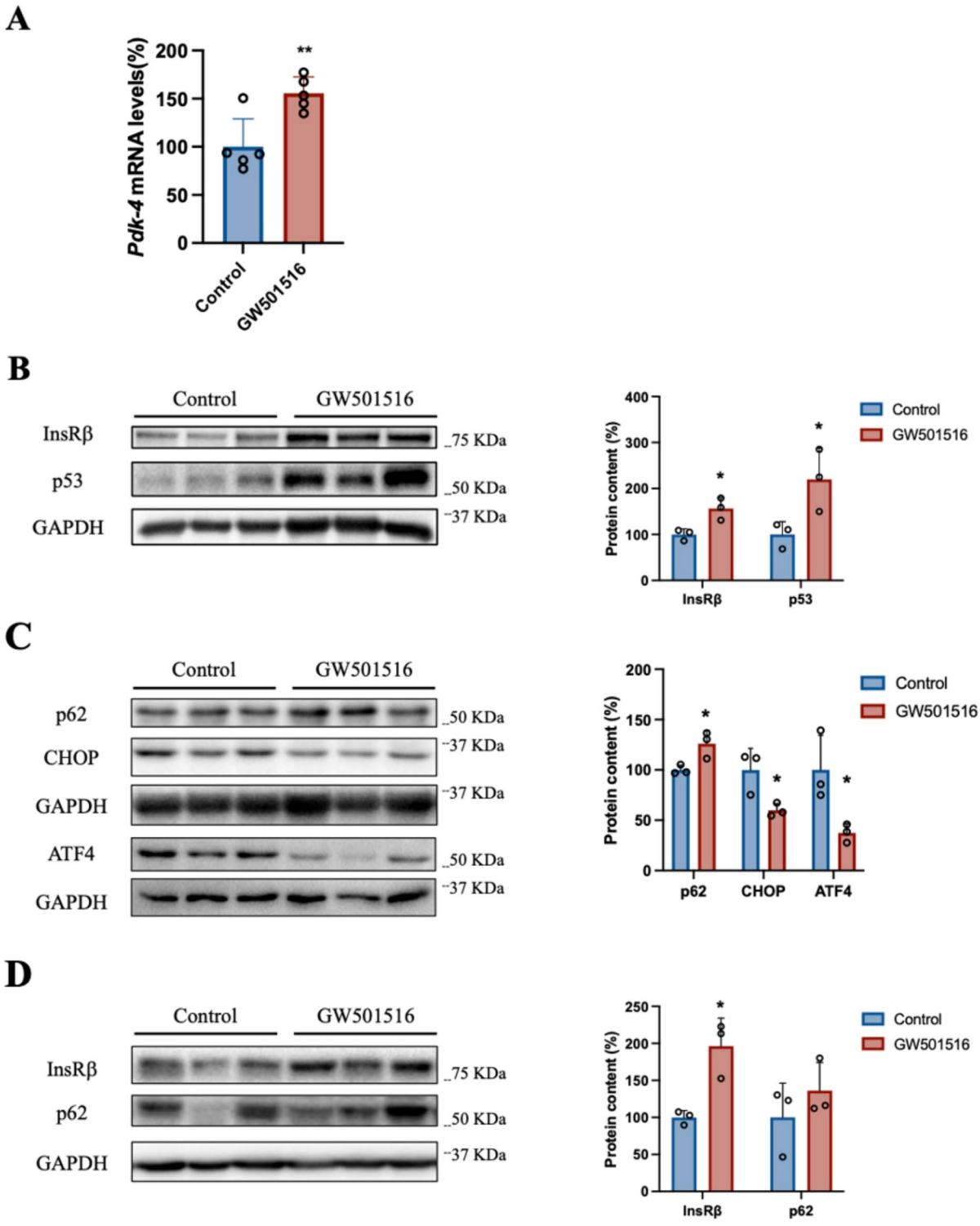

Fig. 2 The PPARβ/δ agonist GW501516 increases InsRβ protein levels in the skeletal muscle of mice. (**A**) mRNA levels of Pdk4in the skeletal muscle of control mice and mice treated with GW501516 for 6 days (n = 5 animals). (**B**) Skeletal muscle cell lysate extracts from control mice and mice treated with GW501516 for 6 days were assayed via western blot analysis with antibodies against InsRβ, p53, or GAPDH ($n = 3$ animals). (**C**) Western blot analysis with antibodies against p62, CHOP, ATF4, or GAPDH ($n = 3$ animals). (**D**) Epididymal adipose tissue lysate extracts from control mice and mice treated with GW501516 for 6 days were assayed via western blot analysis with antibodies against InsRβ, p62, or GAPDH ($n = 3$ animals). Data are presented as the mean ± SD. *$p < 0.05$, **$p < 0.01$, and ***$p < 0.001$ *versus* control. *p*-values were determined by two-tailed unpaired Student's t-test

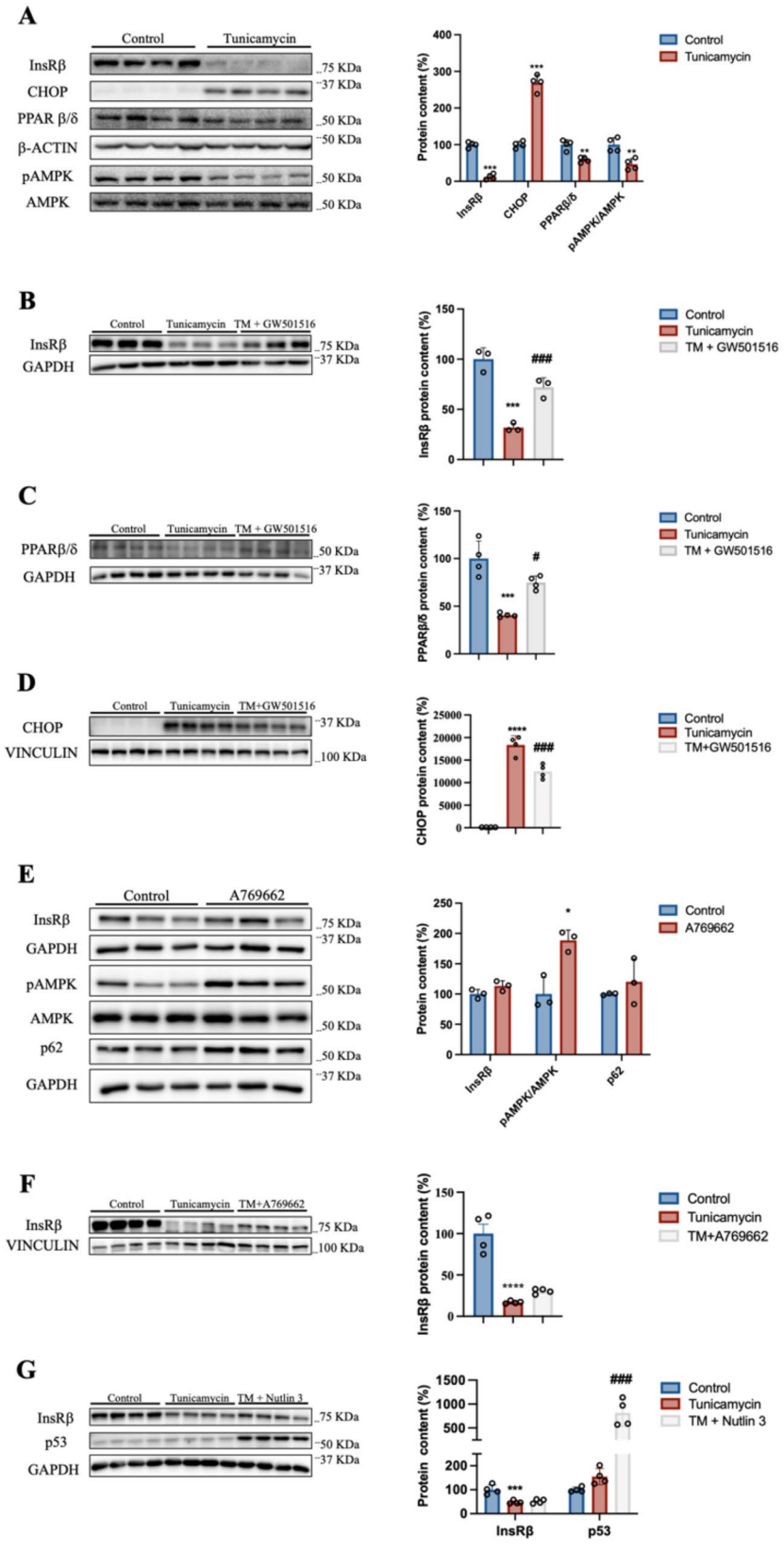

Fig. 3 (See legend on next page.)

(See figure on previous page.)

Fig. 3 Tunicamycin reduces InsRβ protein levels in C2C12 myotubes and GW501516 reverses this reduction. (**A**) Western blot analysis with antibodies against InsRβ, CHOP, PPARβ/δ, phosphorylated and total AMPK, or β-actin in C2C12 myotubes exposed to 5 μg/mL of tunicamycin (TM) for 24 h. (**B**) InsRβ protein levels in C2C12 myotubes exposed to TM (0.1 μg/mL) in the presence or absence of 10 μM of the PPARβ/δ agonist GW501516 for 24 h. (**C**) PPARβ/δ and (**D**) CHOP protein levels in C2C12 myotubes exposed to TM (0.1 μg/mL) in the presence or absence of 10 μM of GW501516 for 24 h. (**E**) InsRβ, p62 and phosphorylated and total AMPK protein levels in C2C12 myotubes exposed to 60 μM of the AMPK activator A769662 for 16 h. (**F**) InsRβ protein levels in C2C12 myotubes exposed to TM (0.1 μg/mL) in the presence or absence of 60 μM of A769662 for 24 h. (**G**) InsRβ, p53, and GAPDH protein levels in C2C12 myotubes exposed to TM (0.1 μg/mL) in the presence or absence of 10 μM of the p53 inducer nutlin-3 for 24 h. Data are presented as the mean ± SD. $^{*}p < 0.05$ and $^{***}p < 0.001$ *versus* control. $^{\#\#}p < 0.01$ and $^{\#\#\#}p < 0.001$ *versus* TM. *p*-values were determined by two-tailed unpaired Student's t-test or ANOVA with Tukey's post-hoc test

its protective effect on InsRβ protein levels in tunicamycin-exposed cells. Altogether, these findings suggest that PPARβ/δ activation prevents the ER stress-mediated reduction in the protein levels of the InsRβ by blunting its lysosomal degradation.

PPARβ/δ regulates EphB4

EphB4 directly binds to the InsRβ and this interaction facilitates clathrin-mediated InsRβ endocytosis and degradation in lysosomes [8]. When we evaluated the levels of this protein in the skeletal muscles of *Ppard*$^{-/-}$ mice, we observed a slight but significant increase in EphB4 protein levels when compared to WT mice (Fig. 5A). In line with these observations, treatment of WT mice with the PPARβ/δ agonist GW501516 decreased EphB4 protein levels in their skeletal muscle (Fig. 5B). In C2C12 myotubes, chloroquine did not affect the increase in CHOP protein levels caused by tunicamycin (Fig. 5C), suggesting that a reduction in ER stress is not involved in the effects of this compound on InsRβ levels. By contrast, chloroquine reduced the protein levels of EphB4 (Fig. 5C). These findings suggest that the inhibition of lysosomal activity caused by PPARβ/δ activation and chloroquine contributes to the upregulation of the InsRβ by reducing its EphB4-mediated degradation in lysosomes [8].

Discussion

The accumulation of unfolded and partially folded proteins in the ER activates a signaling network termed the unfolded protein response. This adaptive response is linked to different processes that are involved in the development of insulin resistance and T2DM, including inflammation, lipid accumulation, insulin biosynthesis, and β-cell apoptosis [26]. In obese patients, ER stress is present in several organs [27, 28]. Moreover, patients with impaired glucose tolerance and overt T2DM show an approximately 50% reduction in the InsR level, with this deficiency contributing to the inhibition of insulin signaling [29–31]. ER stress downregulates InsR levels [6] and the amount of this receptor that reaches the plasma membrane [7]. Therefore, deciphering the mechanisms involved in the ER stress-mediated downregulation of InsR and the potential targets to prevent this reduction can provide new strategies for the prevention and treatment of insulin resistance and T2DM. We, herein, identified that PPARβ/δ regulates InsRβ protein levels of in skeletal muscle. In fact, our findings show that InsRβ protein levels are reduced in the skeletal muscle of *Ppard*$^{-/-}$ mice, whereas WT mice treated with the PPARβ/δ agonist GW510156 display increased InsRβ levels in their skeletal muscle. We [11] and others [12] have previously reported that PPARβ/δ activation increases InsR levels in the skeletal muscle and adipocytes, respectively. However, the mechanisms involved remained unknown. In the present study, the reduction in InsRβ in the skeletal muscle of *Ppard*$^{-/-}$ mice was found to be associated with an increase in the levels of the ER stress marker CHOP, with GW501516 reducing the protein levels of CHOP and ATF4 in skeletal muscle. In addition, GW501516 partially reversed the reduction in InsRβ levels caused by the ER stressor tunicamycin and attenuated the increase in CHOP levels in C2C12 myotubes. Since InsR levels have been reported to be negatively associated with CHOP levels in the insulin target tissues of *db/db* mice and HFD-fed mice [6], these findings suggest that the inhibitory effect of PPARβ/δ on ER stress [24] is involved in these changes (Fig. 6).

Besides ER stress, another factor contributing to the reduction in InsRβ levels is hyperinsulinemia [5, 8]. In fact, hyperinsulinemia causes an increase in the lysosomal degradation of the InsRβ [5]. Consistent with this, we observed that inhibition of the lysosomal degradation by chloroquine nearly completely reverted the reduction in InsRβ levels caused by tunicamycin. This suggests that the ER stress-mediated degradation of the InsRβ ultimately involves increasing its lysosomal degradation. Lysosomal degradation can be monitored by measuring the protein levels of p62, which is degraded via autophagy and lysosomal pathways [23]. Along this line, chloroquine increased the protein levels of p62 in C2C12 myotubes exposed to tunicamycin. Interestingly, since we observed an increase in p62 levels in C2C12 myotubes treated with GW501516, we hypothesized that PPARβ/δ activation might affect lysosomal activity. In fact, our findings show that tunicamycin increases lysosomal activity in C2C12 myotubes, but co-incubation with GW501516 reverses this increase. A previous study reported that the PPARβ/δ agonist HPP593 increases the accumulation of the p62 protein in the kidneys of rats [32], supporting

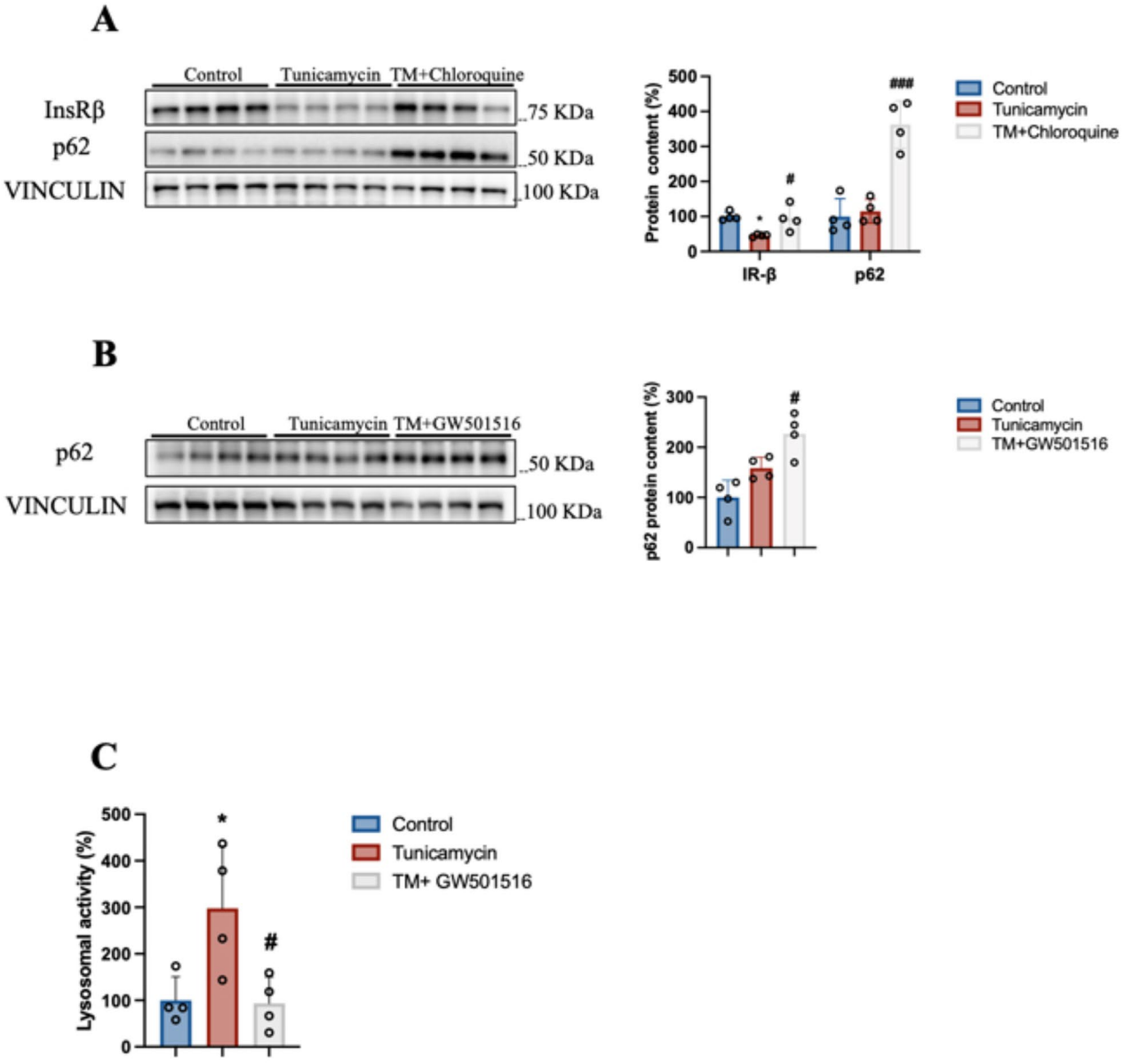

Fig. 4 The PPARβ/δ agonist GW501516 prevents the increase in lysosomal activity caused by exposure to tunicamycin in C2C12 myotubes. A) Western blot analysis with antibodies against InsRβ or p62 in C2C12 myotubes exposed to 0.1 μg/mL of tunicamycin (TM) in the presence or absence of 50 μM of chloroquine, an inhibitor of lysosomal degradation, for 24 h. (**B**) p62 protein levels in C2C12 myotubes exposed to TM (0.1 μg/mL) in the presence or absence of 10 μM of the PPARβ/δ agonist GW501516 for 24 h. (**C**) Lysosomal activity in C2C12 myotubes exposed to TM (0.1 μg/mL) in the presence or absence of 10 μM of GW501516 for 24 h. Data are presented as the mean ± SD. *$p < 0.05$ and ***$p < 0.001$ *versus* control. $^{\#\#}p < 0.01$ and $^{\#\#\#}p < 0.001$ *versus* TM. *p*-values were determined by ANOVA with Tukey's post-hoc test

a role for PPARβ/δ in lysosomal activity. Therefore, our findings suggest that PPARβ/δ activation prevents ER stress-mediated InsRβ degradation by reducing both ER stress and lysosomal degradation.

The findings of the present study discard the involvement of AMPK and p53 in the beneficial effect of PPARβ/δ activation on ER stress-mediated InsRβ degradation. Although many of the metabolic effects of PPARβ/δ agonists are mediated by AMPK [26], the AMPK activator A769662 did not significantly restore InsRβ levels in the cells exposed to tunicamycin. PPARβ/δ agonists can increase the levels of p53 via AMPK [11], while p53 has been reported to increase InsR expression [22]. However, the upregulation of p53 levels by treating C2C12 cells with nutlin-3 did not restore InsRβ levels in the cells exposed to tunicamycin.

Hyperinsulinemia induces InsRβ degradation in the liver through EphB4 [8]. This tyrosine kinase receptor

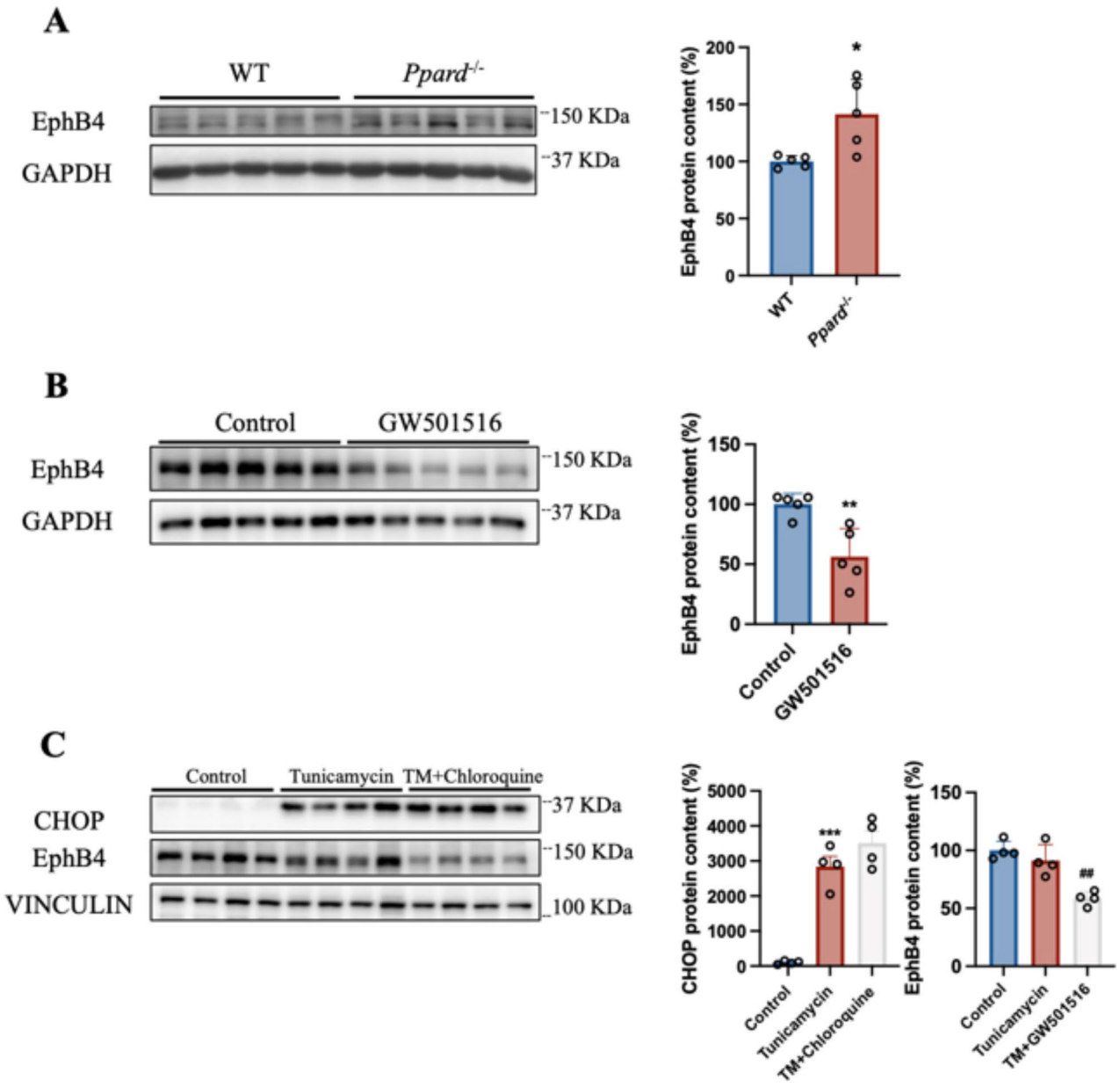

Fig. 5 PPARβ/δ activation reduces the protein levels of EphB4 in C2C12 myotubes. (**A**) Skeletal muscle cell lysate extracts from *Ppard*$^{-/-}$ and WT mice were assayed via western blot analysis with antibodies against EphB4 or GAPDH ($n = 5$ animals). (**B**) Skeletal muscle cell lysate extracts from control mice and mice treated with GW501516 for 6 days were assayed via western blot analysis with antibodies against EphB4 or GAPDH ($n = 5$ animals). (**C**) CHOP and EphB4 protein levels in C2C12 myotubes exposed to 0.1 μg/mL of tunicamycin (TM) in the presence or absence of 50 μM of chloroquine, an inhibitor of lysosomal degradation, for 24 h. Data are presented as the mean ± SD. *$p < 0.05$ and ***$p < 0.001$ *versus* control. $^{\#\#}p < 0.01$ and $^{\#\#\#}p < 0.001$ *versus* TM. *p*-values were determined by ANOVA with Tukey's post-hoc test or by two-tailed unpaired Student's t-test

binds to the InsRβ, which facilitates the endocytosis of the InsRβ and its degradation in lysosomes. Consistent with this, the inhibition of lysosomal degradation reversed the effect of EphB4 overexpression on InsRβ levels. These findings indicate that the modulation of EphB4 levels impacts InsRβ degradation. Interestingly, in the present study, *Ppard*$^{-/-}$ mice displayed higher levels of EphB4 in the skeletal muscle compared to WT mice, while treatment of the WT mice with GW501516 reduced EphB4 protein levels. These data suggest that the reduction in InsRβ degradation caused by the activation of PPARβ/δ may also involve a decrease in EphB4 levels, thereby attenuating the transport of the InsRβ to the lysosomes for degradation. However, how PPARβ/δ regulates EphB4 still needs to be clarified in future studies with larger cohorts of mice. Therefore, a limitation of this

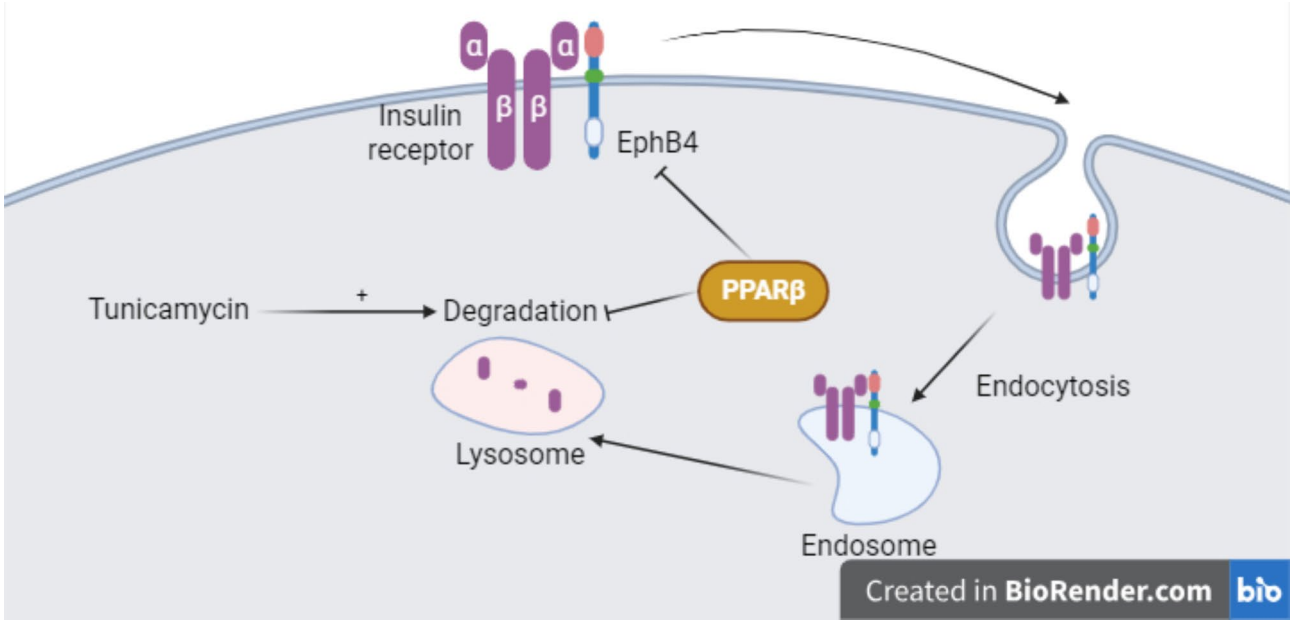

Fig. 6 Proposed mechanistic model in which PPARβ/δ activation prevents the ER stress-mediated reduction in InsRβ levels by attenuating both ER stress and the increase in lysosomal activity as well as by reducing EphB4 levels

study is that we have not provided the specific molecular mechanism involved in the regulation of EphB4 by PPARβ/δ.

Conclusions

Collectively, the findings of this study highlight a novel regulatory mechanism in which PPARβ/δ activation prevents the ER stress-mediated reduction in InsRβ levels by attenuating both ER stress and the increase in lysosomal activity as well as by reducing EphB4 levels.

Abbreviations

ATF4	Activating transcription factor 4
CHOP	C/EBP homologous protein
EphB4	Ephrin receptor B4
HFD	High-fat diet
MDM2	Murine double minute 2
NQO1	NAD(P)H: quinone oxidoreductase 1
Nrf2	Nuclear factor erythroid-2-related factor 2
PPAR	Peroxisome proliferator-activated receptor
T2DM	Type 2 diabetes mellitus
WT	Wild-type

Supplementary Information

The online version contains supplementary material available at https://doi.org/10.1186/s12964-024-01972-5.

Supplementary Material 1: **Supplementary Fig. 1**. Cell viability analysis assessed by MTT in C2C12 myotubes exposed to 10 μM of GW501516, 0.1 μg/mL of tunicamycin (TM), 50 μM of chloroquine, 60 μM A769662 or their combination for 24 h. Data are presented as the mean ± SD.

Supplementary Material 2: **Supplementary Table 1.** Primer sequences.

Supplementary Material 3

Acknowledgements

We would like to thank the Language Services of the University of Barcelona for revising the manuscript.

Author contributions

"JJA, JRW, EB, and MVC designed the experiments. JJA, JRW, EB and MVC performed the experiments. JJA, JRW, EB, AC, WW, XP, and MVC analyzed the data, reviewed the results, and prepared the manuscript. MVC is the guarantor of this work and, as such, has full access to all the data in the study and takes responsibility for the integrity of the data and the accuracy of the data analysis."

Funding

This study was partly supported by the grant PID2021-122116OB-I00 from the MICIU/AEI/https://doi.org/10.13039/501100011033 and "ERDF, A Way of making Europe". CIBER de Diabetes y Enfermedades Metabólicas Asociadas (CIBERDEM) is a Carlos III Health Institute project. Support was also received from the CERCA Programme/Generalitat de Catalunya. E.B is a Serra Hunter fellow.

Data availability

No datasets were generated or analysed during the current study.

Declarations

Consent for publication

Not applicable.

Competing interests

The authors declare no competing interests.

Received: 22 August 2024 / Accepted: 30 November 2024
Published online: 18 December 2024

References

1. Batista TM, et al. Defining the underlying defect in insulin action in type 2 diabetes. Diabetologia. 2021;64:994–1006. https://doi.org/10.1007/s00125-021-05415-5.

2. DeFronzo RA, Tripathy D. Skeletal muscle insulin resistance is the primary defect in type 2 diabetes. Diabetes Care. 2009;32(Suppl 2):157–63. https://doi.org/10.2337/dc09-S302.
3. Rowland AF, et al. Mapping insulin/GLUT4 circuitry. Traffic. 2011;12:672–81. https://doi.org/10.1111/j.1600-0854.2011.01178.x.
4. Frojdo S, et al. Alterations of insulin signaling in type 2 diabetes: a review of the current evidence from humans. Biochim Biophys Acta. 2009;1792:83–92. https://doi.org/10.1016/j.bbadis.2008.10.019.
5. Lay AC, et al. Prolonged exposure of mouse and human podocytes to insulin induces insulin resistance through lysosomal and proteasomal degradation of the insulin receptor. Diabetologia. 2017;60:2299–311. https://doi.org/10.1007/s00125-017-4394-0.
6. Zhou L, et al. Autophagy-mediated insulin receptor down-regulation contributes to endoplasmic reticulum stress-induced insulin resistance. Mol Pharmacol. 2009;76:596–603. https://doi.org/10.1124/mol.109.057067.
7. Brown M, et al. Endoplasmic reticulum stress causes insulin resistance by inhibiting delivery of newly synthesized insulin receptors to the cell surface. Mol Biol Cell. 2020;31:2597–629. https://doi.org/10.1091/mbc.E18-01-0013.
8. Liu X, et al. Insulin induces insulin receptor degradation in the liver through EphB4. Nat Metab. 2022;4:1202–13. https://doi.org/10.1038/s42255-022-00634-5.
9. Vazquez-Carrera M. Unraveling the effects of PPARbeta/delta on insulin resistance and Cardiovascular Disease. Trends Endocrinol Metab. 2016;27:319–34. https://doi.org/10.1016/j.tem.2016.02.008.
10. Schuler M, et al. PGC1alpha expression is controlled in skeletal muscles by PPARbeta, whose ablation results in fiber-type switching, obesity, and type 2 diabetes. Cell Metab. 2006;4:407–14. https://doi.org/10.1016/j.cmet.2006.10.003.
11. Aguilar-Recarte D, et al. GDF15 mediates the metabolic effects of PPARbeta/delta by activating AMPK. Cell Rep. 2021;36:109501. https://doi.org/10.1016/j.celrep.2021.109501.
12. Kim WJ, et al. PPARbeta/delta agonist GW501516 inhibits TNFalpha-induced repression of adiponectin and insulin receptor in 3T3-L1 adipocytes. Biochem Biophys Res Commun. 2019;510:621–8. https://doi.org/10.1016/j.bbrc.2019.02.013.
13. Montori-Grau M, et al. Endoplasmic reticulum stress downregulates PGC-1alpha in skeletal muscle through ATF4 and an mTOR-mediated reduction of CRTC2. Cell Commun Signal. 2022;20. https://doi.org/10.1186/s12964-022-00865-9.
14. Tanaka T, et al. Activation of peroxisome proliferator-activated receptor delta induces fatty acid beta-oxidation in skeletal muscle and attenuates metabolic syndrome. Proc Natl Acad Sci U S A. 2003;100:15924–9. https://doi.org/10.1073/pnas.0306981100.
15. Zhang M, et al. PPARbeta/delta attenuates hepatic fibrosis by reducing SMAD3 phosphorylation and p300 levels via AMPK in hepatic stellate cells. Biomed Pharmacother. 2024;179:117303. https://doi.org/10.1016/j.biopha.2024.117303.
16. Mauthe M, et al. Chloroquine inhibits autophagic flux by decreasing autophagosome-lysosome fusion. Autophagy. 2018;14:1435–55. https://doi.org/10.1080/15548627.2018.1474314.
17. Jurado-Aguilar J, et al. GDF15 activates AMPK and inhibits gluconeogenesis and fibrosis in the liver by attenuating the TGF-beta1/SMAD3 pathway. Metabolism. 2024;152:155772. https://doi.org/10.1016/j.metabol.2023.155772.
18. Barroso E, et al. PPARbeta/delta ameliorates fructose-induced insulin resistance in adipocytes by preventing Nrf2 activation. Biochim Biophys Acta. 2015;1852:1049–58. https://doi.org/10.1016/j.bbadis.2015.02.010.
19. Di Francesco A, et al. NQO1 protects obese mice through improvements in glucose and lipid metabolism. NPJ Aging Mech Dis. 2020;6. https://doi.org/10.1038/s41514-020-00051-6.
20. Dong L, et al. SMURF1 attenuates endoplasmic reticulum stress by promoting the degradation of KEAP1 to activate NRF2 antioxidant pathway. Cell Death Dis. 2023;14:361. https://doi.org/10.1038/s41419-023-05873-2.
21. Moruzzi N, et al. Tissue-specific expression of insulin receptor isoforms in obesity/type 2 diabetes mouse models. J Cell Mol Med. 2021;25:4800–13. https://doi.org/10.1111/jcmm.16452.
22. Sarfstein R, Werner H. Tumor suppressor p53 regulates insulin receptor (INSR) gene expression via direct binding to the INSR promoter. Oncotarget. 2020;11:2424–37. https://doi.org/10.18632/oncotarget.27645.
23. Rusten TE, Stenmark H. p62, an autophagy hero or culprit? Nat Cell Biol. 2010;12:207–9. https://doi.org/10.1038/ncb0310-207.
24. Salvado L, et al. PPARbeta/delta prevents endoplasmic reticulum stress-associated inflammation and insulin resistance in skeletal muscle cells through an AMPK-dependent mechanism. Diabetologia. 2014;57:2126–35. https://doi.org/10.1007/s00125-014-3331-8.
25. Sparks A, et al. The degradation of p53 and its major E3 ligase Mdm2 is differentially dependent on the proteasomal ubiquitin receptor S5a. Oncogene. 2014;33:4685–96. https://doi.org/10.1038/onc.2013.413.
26. Salvado L, et al. Targeting endoplasmic reticulum stress in insulin resistance. Trends Endocrinol Metab. 2015;26:438–48. https://doi.org/10.1016/j.tem.2015.05.007.
27. Ozcan U, et al. Endoplasmic reticulum stress links obesity, insulin action, and type 2 diabetes. Science. 2004;306:457–61. https://doi.org/10.1126/science.1103160.
28. Boden G, et al. Increase in endoplasmic reticulum stress-related proteins and genes in adipose tissue of obese, insulin-resistant individuals. Diabetes. 2008;57:2438–44. https://doi.org/10.2337/db08-0604.
29. Olefsky JM, Reaven GM. Insulin binding in diabetes. Relationships with plasma insulin levels and insulin sensitivity. Diabetes. 1977;26:680–8. https://doi.org/10.2337/diab.26.7.680.
30. Kolterman OG, et al. Receptor and postreceptor defects contribute to the insulin resistance in noninsulin-dependent diabetes mellitus. J Clin Invest. 1981;68:957–69. https://doi.org/10.1172/jci110350.
31. Kolterman OG, et al. Mechanisms of insulin resistance in human obesity: evidence for receptor and postreceptor defects. J Clin Invest. 1980;65:1272–84. https://doi.org/10.1172/JCI109790.
32. Fedorova LV, et al. Peroxisome proliferator-activated receptor delta agonist, HPP593, prevents renal necrosis under chronic ischemia. PLoS ONE. 2013;8:e64436. https://doi.org/10.1371/journal.pone.0064436.

Publisher's note